Absolute cross section for $Si^{2+}(3s3p\ ^3P^o \rightarrow 3s3p\ ^1P^o)$ electron-impact excitation

P. H. Janzen, L. D. Gardner, D. B. Reisenfeld,* and J. L. Kohl
Harvard-Smithsonian Center for Astrophysics, Cambridge, Massachusetts 02138
(Received 3 November 2002; published 13 May 2003)

We have measured the absolute energy-averaged cross section for electron-impact excitation of $Si^{2+}(3s3p\ ^3P^o \rightarrow 3s3p\ ^1P^o)$ from energies below threshold to the turn-on of the $3s3p\ ^3P^o \rightarrow 3p^2\ ^3P$ transition. A beams modulation technique with inclined electron and ion beams was used. Radiation at 120.65 nm from the decay of the excited ions to the $3s^2\ ^1S$ ground state was detected using an absolutely calibrated optical system. The fractional population of metastable $Si^{2+}(3s3p\ ^3P^o)$ in the incident ion beam was determined to be $0.256 \pm 0.035 (1.65\sigma)$. The experimental energy spread ranged from 0.85 eV (full width at half maximum) at the lowest energies to 0.56 eV at the highest. Resonance features consistent with 12-state close-coupling *R*-matrix calculations are seen.

DOI: 10.1103/PhysRevA.67.052702 PACS number(s): 34.80.Kw, 34.80.Lx

I. INTRODUCTION

Electron-impact excitation (EIE) is the dominant mechanism for the formation of emission lines in many laboratory and astrophysical plasmas. Intensities of spectral lines arising from EIE can provide diagnostics of the temperature and density of an emitting plasma, and of the abundance of elements in the plasma. Si^{2+} has particular astrophysical importance: the 120.65-nm $^1P^o \rightarrow {}^1S$ line has been observed in stellar plasmas [1], the solar transition region [2], and coronal mass ejections [3]. Excitations to and from the low-lying $3s3p\ ^3P^o$ metastable term (see Fig. 1) give rise to several emission lines that, when measured in comparison to the 120.65 nm line, have made Si^{2+} an extensively utilized electron-density diagnostic [4,5].

Although density diagnostics require accurate knowledge of the cross section for EIE out of metastable levels, few absolute measurements of such cross sections have been attempted. Crandall *et al.* performed an experiment to measure EIE in Hg^+ for which they saw $5d^9 6s^2\ ^2D \rightarrow 6p\ ^2P^o_{3/2}$ excitation; however, the fraction of ^2D metastables in their ion beam was not known well enough to provide a meaningful absolute cross section [6]. More recently, Reisenfeld *et al.* measured the cross section for $Si^{2+}(3s3p\ ^3P^o \rightarrow 3p^2\ ^3P)$ excitation, primarily to remove its contribution for a measurement of the $3s^2\ ^1S \rightarrow 3s3p\ ^1P^o$ EIE cross section [7]. No effort was made to achieve better statistical uncertainty than necessary for this subtraction. Bannister *et al.* performed near-threshold measurements of the $2s2p\ ^3P^o \rightarrow 2p^2\ ^3P$ excitation in metastable C^{2+} and the sum of the two spin-forbidden excitations $2s^2\ ^1S \rightarrow 2s2p\ ^3P^o$ and $2s2p\ ^3P^o \rightarrow 2s2p\ ^1P^o$, which were not separately resolvable by their experimental technique, in C^{2+} and O^{4+}. However, they did not directly measure their metastable fractions and instead assumed fractions similar to those extracted from a different electron-cyclotron resonance (ECR) ion source running the same gases [8].

Electron-impact excitation cross sections that are dominated by autoionizing resonances, such as spin-forbidden transitions, are particularly difficult to calculate theoretically because the size of an individual resonance is extremely sensitive to the strength of the coupling to neighboring resonances [9]. Agreement between theory and previous experiments that resolve resonance structure has been mixed (e.g., Refs. [10–12,7,8]), and more experimental benchmark measurements are needed.

Previous EIE measurements of an ion involving an electron spin flip have dealt with transitions from the ground state, usually to the lowest-lying metastable state. Photon

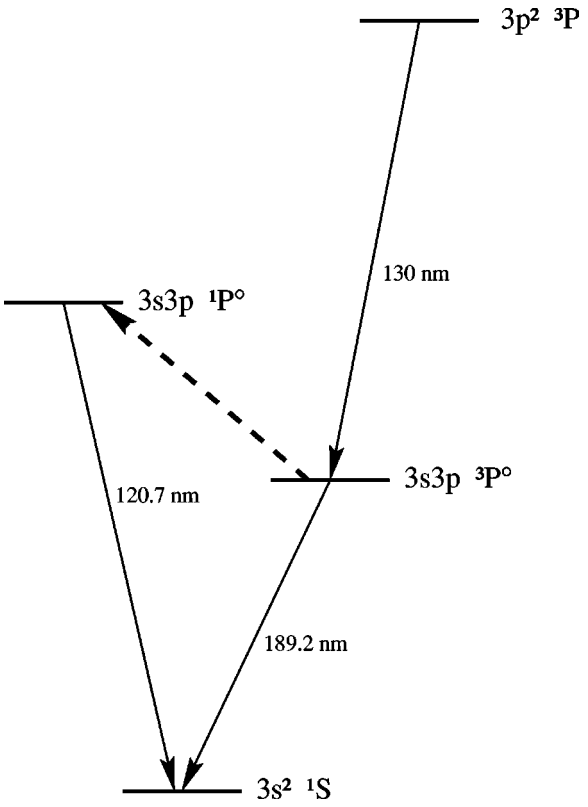

FIG. 1. Partial term diagram for Si^{2+}. The excitation under study is shown by a dashed line.

*Present address: Los Alamos National Laboratory, M/S-D466, Los Alamos, NM 87545.

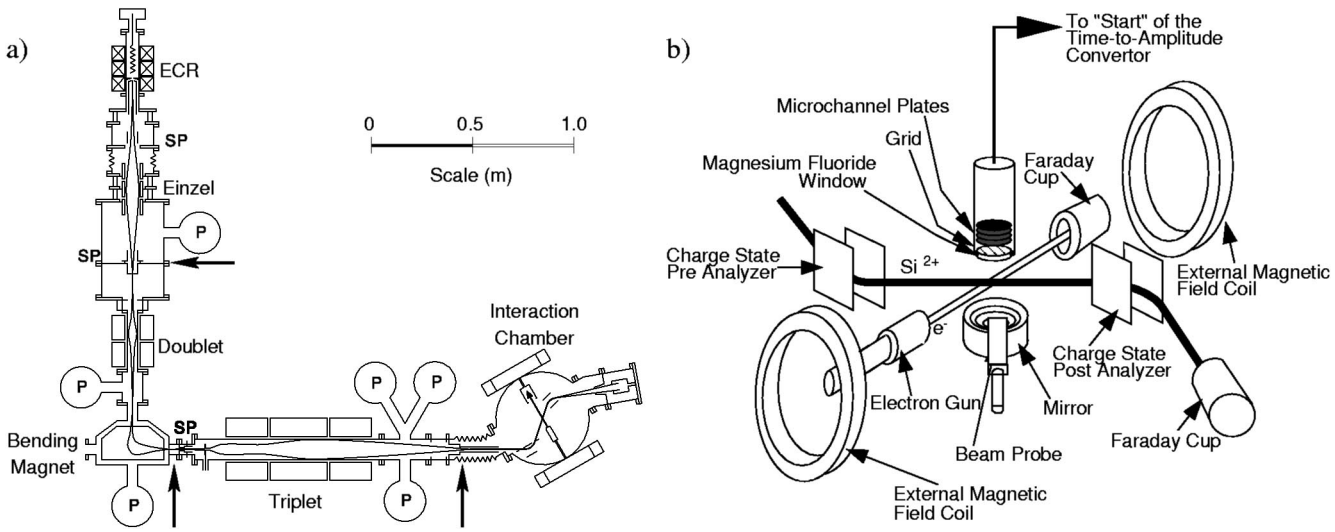

FIG. 2. Diagram of the experimental apparatus. (a) Overview. Pumps are indicated by *P* and steering plates by *SP*. Arrows point to differential pumping apertures. Beam attenuation was performed by leaking H_2 or Ar into the triplet region. (b) The interior of the interaction chamber.

detection techniques are clearly not suited to measure EIE to metastable states unless the excited state is quenched somehow, and most such measurements have detected the inelastically scattered electrons instead. However, spin-forbidden transitions *from* a metastable state to one that can decay via a dipole transition to the ground state can be measured by observing decay photons. In the case under study, metastable Si^{2+} $^3P^o$ ions excited to the $^1P^o$ levels decay to the ground state with a lifetime of 0.38 ns [13]. We have used the photon detection technique to measure the EIE cross section for the $3s3p\,^3P^o \rightarrow 3s3p\,^1P^o$ transition.

II. MEASUREMENTS

A. Apparatus and technique

The experiment was performed by measuring the light emitted from ions excited by electron impact. The apparatus and technique are discussed in Reisenfeld *et al.* [7]. Briefly, a carefully prepared beam of Si^{2+} ions, generated in an ECR ion source and extracted at 10 kV, is crossed with an electron beam at 45° [see Fig. 2(a)]. Typical ion current was 24 nA and typical electron current was 30–50 μA, depending on collision energy. A 1–1.5-mT magnetic field is applied coaxially with the electron beam to collimate it and to increase its density. The shape and current of both beams are measured. Photons are counted using beam chopping and synchronous detection to subtract background. A large mirror subtending slightly over π steradians (sr) below the collision volume concentrates photons onto a KBr-coated microchannel plate detector (MCP), which itself subtends 0.32 sr [see Fig. 2(b)]. The KBr coating allowed good detection efficiency at 120.65 nm without increasing the MCP's sensitivity to 189.2-nm metastable decay photons, which are a background when measuring EIE. Optical elements were calibrated separately and a three-dimensional ray-tracing code, which modeled all optical elements and the effects of multiple reflections between partially reflecting objects, was used to determine the overall absolute photon detection efficiency of the system. The absolute detected quantum efficiency of the MCP was determined by referencing to a CsTe photodiode calibrated by the National Institute of Standards and Technology (NIST). All calibrations were performed at 120 nm and 121.6 nm and interpolated to 120.65 nm.

Absolute measurement of the $^3P^o \rightarrow {}^1P^o$ EIE cross section required accurate knowledge of the metastable fraction. Also, with the smaller fraction and smaller cross section than the $^1S \rightarrow {}^1P^o$ excitation, which was previously measured with the same apparatus, came a lower signal-to-background ratio and the need for longer data collection times: typical signal rates were 2 s^{-1} on a background of a few hundred per second. Finally, the $^3P^o \rightarrow {}^1P^o$ excitation threshold, 3.72 eV in the center-of-mass (c.m.) frame [14], requires a beam of electrons with energies $\sim$5.4 eV in the lab frame.

B. Determination of the metastable fraction

The fraction of Si^{2+} ions in the metastable $3s3p\,^3P^o$ state in the collision volume was only about 26%. Various techniques have been devised to determine the metastable fraction of an ion beam [15,16]. Two methods were used in this experiment: the beam attenuation method, in which the difference in attenuation cross sections between the metastable state and the ground state is used to tell them apart; and the decay-photon method [17], in which light arising from the decay of the metastable level is observed.

Beam attenuation in fast ion beams is a well-established technique for determining metastable fraction [18]. A single-species ion beam passing through a gas thickness $x = nL$, where n is the gas density and L is its length, will be attenuated by a factor $e^{-\sigma x}$, where σ is the attenuation coefficient, arising principally from electron capture (for multiply charged ions, ions that change charge state must be removed from the beam). If the beam is composed of two compo-

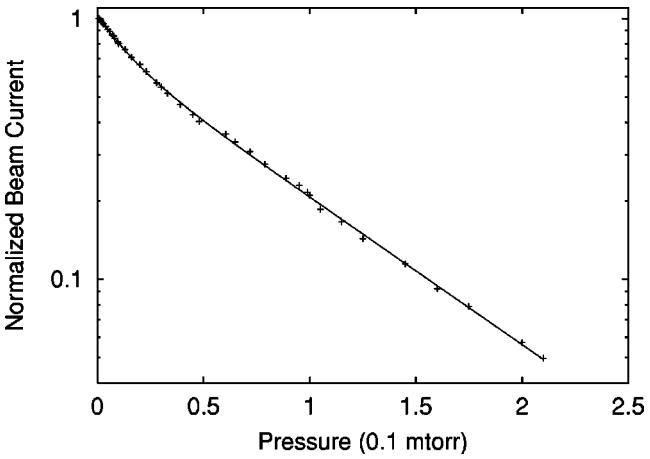

FIG. 3. Transmitted Si^{2+} current vs H_2 Bayard-Alpert ion gauge pressure for one H_2 run. The solid line is a two-exponential fit.

nents, ground-state ions and a fraction f of metastables, with attenuation cross sections σ and σ^*, respectively, the current passing through will be

$$I(x)=I_0((1-f)e^{-\sigma x}+fe^{-\sigma^* x}). \quad (1)$$

The fraction of metastables can then be accurately determined, if σ and σ^* are sufficiently different, by measuring transmitted current as a function of pressure. Difficulties arise if ions that interact with the attenuating gas are not removed from the beam: in particular, if a metastable ion can collisionally deexcite without altering its trajectory, then the two-exponential fit of Eq. (1) will yield an erroneously low apparent fraction f. Since the cross sections for electron capture and for collisional deexcitation depend on the choice of attenuating gas, this effect can be investigated by using a variety of gases.

The region used for attenuation was between two differential pumping apertures, which were roughly 1.5 m apart and were located between the bending magnet and the interaction chamber [see Fig. 2(a)]. Pressure in the attenuation region varied with the distance to the pumping apertures and from the gas leak, near which the pressure was monitored. Throughout the attenuation region, a magnetic quadrupole triplet lens focuses the Si^{2+} beam through the exit differential pumping nozzle, which leads to the interaction chamber. In the interaction chamber, the beam is electrostatically separated by a preanalyzer and then again by a postanalyzer [see Fig. 2(b)] before the remaining Si^{2+} enters a Faraday cup.

Prior to the EIE measurements, Ar and H_2 were used independently as attenuating gases; afterwards, H_2 was used again. A sample H_2 run is shown in Fig. 3; the fit assumes constant fractional uncertainty in the current measurements. The H_2 results before and after are reasonably consistent ($f=0.251\pm0.007$ and $f=0.266\pm0.008$, where the listed 1σ uncertainties arise from the fit covariance matrices, and multiple runs have been averaged together) as are the values of f for Ar and H_2 (0.275 ± 0.01 and 0.257 ± 0.006), although there is the suggestion of a slight difference, possibly due to collisional deexcitation. At some of the higher attenuation gas pressures, particularly with H_2, the pressure in the ion source was seen to increase slightly, as inferred from its total output current; however, the metastable fraction determined was insensitive to the removal of the highest-pressure points from the fit. The ratio of attenuation coefficients was $\sigma^*/\sigma=5.0$ for H_2 and $\sigma^*/\sigma=3.9$ for Ar.

The metastable fraction as determined by beam attenuation, averaging all the runs, is $f=0.262\pm0.005$ if the uncertainty is entirely described by the fit covariance matrix. However, uncertainty in the accuracy of pressure measurements, including up to $\pm5\%$ nonlinearity in the ionization gauge reading [19], increases the 90% uncertainty to 0.035. Finally, since f is being measured in the triplet and not in the interaction region, a correction must be made for additional radiative metastable decay during the time the ion beam continues to the interaction region ($\sim3.4\ \mu$s). Principally, it is the $J=1$ level that will decay, which with its measured $59.9\pm3.6\ \mu$s mean lifetime [20] decays considerably faster than the $J=2$ and $J=0$ levels. This correction, using the $J=1$ fraction determined below, amounts to a 2% downward shift. Thus, $f=0.256\pm0.035$ at 90% confidence.

The metastable fraction was also studied using the decay-photon method, originally proposed by Lafyatis and Kohl [21]. The intensity of the 189.2-nm metastable decay radiation emitted by the ion beam as it passes through the field of view of the optical system was measured using an absolutely calibrated Thorne EMI 9413 photomultiplier tube. The absolute detection efficiency of the optical system was measured for 189.2 nm light, thereby allowing determination of the absolute number of photons emitted per unit length of beam. Essentially all the radiation is from the $J=1$ level; thus this method measures the fraction of the beam that is in the $J=1$ level, $f_{J=1}$, rather than the entire metastable fraction f. Assuming that the electron density and temperature in the ion source are high enough to populate the fine-structure levels statistically, which is likely, f can be related to $f_{J=1}$ if the depopulation of the $J=1$ level due to decay in the time since its creation in the ECR ion source is taken into account. Unfortunately, although the time an ion takes to travel from the source extraction aperture to the interaction chamber is known accurately ($\sim10\ \mu$s), the average time it takes an ion to drift out of the ECR plasma to the source exit aperture is not. Taking a time comparable to the expected Si^{2+} Bohm diffusion time, 5–20 μs [22], yields $f\approx0.22$–0.29. This is comparable to the fraction determined by beam attenuation.

It is likely that the metastable fraction present in the Si^{2+} beam never varied far from the measured value during the course of the experiment, for the optimal ion source tuning parameters did not change. The ECR ion source, based on a design from the University of Giessen [23], generates its confinement field entirely with permanent magnets. Microwaves are supplied by a stable 2.45 GHz magnetron. The only variable parameters are the gas pressure and the microwave power. The ion source was kept under vacuum continuously from the beginning of the preceding $Si^{2+}(3s^2\ ^1S \rightarrow 3s3p\ ^1P^o)$ measurement to the end of the $^3P^o \rightarrow {}^1P^o$ measurement. During this time, the only gas used in the source was silane (SiH_4), and the source was kept running

nearly continuously. Pressure inside the source during operation was monitored by the total output current of the source; this proved a more consistent measure of the pressure for a given microwave power setting than ionization gauges, which deteriorated rapidly when run in a silane environment. Drift in total output current was typically less than 0.5% over the course of several hours. Si^{2+} current passing through the interaction region, averaged over 50 s, was typically constant to better than 3% absolute over 6000 s, with a standard deviation under 0.7%.

There was a unique combination of ion source pressure, as measured by total output current, and magnetron power, for which the Si^{2+} current was maximized. These parameters were roughly 0.12 mA and 50 W respectively. Over the course of the data collection, roughly 100 days, the Si^{2+} current dropped 20%, linearly with time, most likely due to silicon residue collecting on the walls and antenna of the ion source as well as on the wires in the extraction aperture. Residue was observed on disassembly. However, the uniqueness of the parameters for obtaining the maximum Si^{2+} current remained. When data were being collected, the ion source was tuned to this maximum. Detuning the ion source from this point did affect the metastable fraction: for instance, with the pressure slightly increased, and the microwave power also increased to maximize the Si^{2+} current at this pressure, the total Si^{2+} current was lowered by 12%, and the metastable fraction was 0.31 with an uncertainty from the covariance matrix of ± 0.03. Retuning the ion source to maximize the total Si^{2+} current always caused the metastable fraction to return to the same value, within the uncertainty of the fit.

C. Determination of the EIE event rate

With only the metastable fraction contributing to the signal, the ratio of signal to background was far lower than for previous experiments on this apparatus. This increased the required integration times from 7–15 h to 20–40 h per energy and required close examination to ensure that the background was subtracted correctly.

The beam chopping pattern for the present experiment is shown in Fig. 4. The total chopping pattern was modulated at a frequency of 16.7 kHz. Photons were detected in delayed coincidence with an electronic pulse that signaled the end of the data acquisition chopping pattern. The photons provided the ''start'' pulse for a time-to-amplitude convertor (TAC) and the electronic pulse provided the ''stop.'' Regions of interest (ROIs) were chosen in each of the four modes. Backgrounds produced by the individual beams, and detector background, are removed from the signal by subtracting regions 3 and 1 from the sum of regions 4 and 2.

By running just the ion beam with no electron beam, which should generate no EIE signal, it was found that the ion beam consistently generated a background that extended into the following ROI (R_1), with an amplitude of 0.0047 ± 0.0006 of the ion-beam signal. This background was not obvious when both beams were turned on, since the electron-beam background was substantially larger than the ion-beam background. A background subtraction offset on this scale is

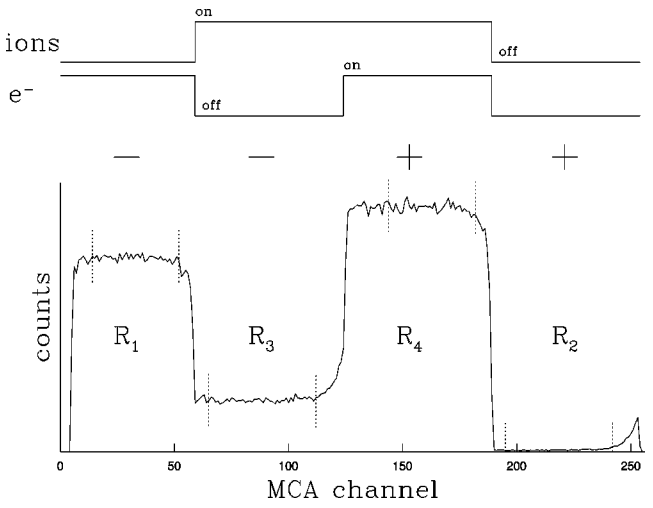

FIG. 4. Chopping pattern used for this experiment (upper) and typical counts for a 3000 s single-energy run (lower), with regions of interest indicated by vertical dotted lines. Note that as the photon signal is used as the start pulse to the time-to-amplitude convertor, time increases to the left. Channels 1–5 are below the multichannel analyzer discriminator setting. The scheme for combining the data is indicated by the plus and minus signs.

not entirely unexpected and could be removed, thereby avoiding the increase in signal uncertainty from the uncertainty in this offset, by using other, more complicated chopping patterns [24]. For this experiment, the effect was measured both before and after the EIE measurement, was found to be independent of the background pressure over the range that data were collected ($1-3\times10^{-10}$ torr), and was subtracted. As a separate test, the electron beam run without the ion beam produced a signal rate consistent with 0, as is expected for the chopping pattern used.

Space-charge modulation of one beam by the other is not expected to create a spurious signal for this experiment as the ion-beam current is too low to affect the magnetically confined electrons significantly. A spurious signal may be generated if gas liberated by either beam changes the background pressure from ROI to ROI. The chopping rate was chosen to be sufficiently high to minimize any such effect. Moreover, particularly near threshold, the electrons are at too low an energy to produce radiation detectable by the MCP except by excitation of a metastable.

Ideally, the count rate is the same in each channel of a given ROI. However, as shown in Fig. 4, the count rate increases over the first few channels when the electron beam is turned on, and decays over the first few channels when the electron beam is turned off (for example, the tail seen in the highest-numbered channels of R_2 carries over from the low-channel end of R_1). At higher energies, such as above the $^1S \rightarrow {}^1P^o$ threshold, this is hidden by a separate pressure-dependent exponential turn-on and turn-off associated with the electron beam exciting a long-lived state in the residual gas of the interaction chamber [22]. The carryover is most likely associated with the electron gun switching electronics and is subtracted correctly as long as the ROIs are all offset consistently from the chopping pattern. This is the case to

within one channel width (0.2 μs), but not necessarily to better than that. The ROIs never start closer than ~ 1 μs to a chopping pattern boundary, to give the beams time to stabilize, so the ranges of time in which the turn-on and decay are largest are not present in the ROIs.

Direct measurement of the linearity of the TAC revealed a drift on the scale of minutes, which unpredictably changed the effective width of the ROIs with respect to each other. The observed drift, coupled with possible effects due to ROIs shifting by some fraction of a channel width from the chopping pattern, introduced an uncertainty in the EIE signal rate of no more than ± 0.29 Hz (90%) over the $\sim$20-h data collection time for each energy. This uncertainty was added in quadrature with the statistical uncertainty of each data point presented here.

Points from the $3s^2\ ^1S \rightarrow 3s3p\ ^1P^o$ excitation were measured before and after the $^3P^o \rightarrow\ ^1P^o$ measurements. These data agreed to within 4%, which is within and comparable to the 1σ statistical error of the measurements, confirming the long-term stability of the detection apparatus.

D. Determination of electron-beam characteristics

The electron gun used for this experiment was designed to produce electron beams at energies of 10 eV or more [21]. The beam current dropped rapidly at lower energies. The $^3P^o \rightarrow\ ^1P^o$ transition has a threshold of 3.72 eV [14], or roughly 5.4 eV in the lab frame. As it was desirable to produce as much electron current as possible to increase the signal count rate, the electron-gun filament was run at a higher current than for the preceding $^1S \rightarrow\ ^1P^o$ measurement of Reisenfeld *et al.*, and magnetic-field confinement was increased. Path-length corrections due to electron spiralling increased to $6 \pm 3\%$ at the lowest energies from $<1\%$ at 8 eV [25]. Beam divergence, as determined from electron-beam probes upstream and downstream from the center of the collision volume, was incorporated into the overlap calculation.

The offset potential of the electron-gun cathode was determined by measuring the $^1S \rightarrow\ ^1P^o$ excitation across threshold. For the electron-gun settings used, the offset was 3.24 ± 0.03 V. Measurements at this threshold were also used to estimate the electron energy spread in the c.m. frame (0.56 ± 0.08 eV). Retarding potential analysis indicated that the energy spread was a function of electron-gun energy for energies below the $^1S \rightarrow\ ^1P^o$ threshold: the energy spread increases at lower V_c as electron spiralling becomes more important. At the lowest energies, retarding potential analysis determined an energy spread of as much as 0.85 ± 0.1 eV full width at half maximum (FWHM) (c.m.), which is consistent with the spread expected from the observed spiralling.

E. Uncertainties

Uncertainty in this experiment was predominantly statistical. Uncertainties in the metastable fraction (14% at 90% confidence) and in the determination of the spatial coordinates of the collision volume, which affects the calculated beam overlap and detection efficiency, were taken to be of random sign and uncorrelated, and were added in quadrature to the statistical error. Systematic uncertainty, which scales all points uniformly, was 12% at 90% confidence: the dominant contributions were the uncertainty in the absolute efficiency of the NIST-calibrated photodiode used to determine the absolute efficiency of the MCP at 120.65 nm (8%), and uncertainties in ion- and electron-beam current measurements (5% each). Other systematic uncertainties were in the amount of nitrogen contamination (N^+) in the ion beam (1%); in drift in the MCP quantum efficiency (2%) and the efficiency of the photodiode used for cross calibration (1%); in radiometric calibration of the window (2%), mirror (3%), MCP (1%), and filters used in calibration (2%); in interpolation from the calibration wavelengths of 120 nm and 121.6 nm to 120.65 nm (2%); and in computational uncertainty in the raytrace (2%) and the overlap determination (1%), where uncertainties are given at a level equivalent to 90% statistical confidence. A detailed discussion of the systematic uncertainties for the similar measurement of the $3s^2\ ^1S \rightarrow 3s3p\ ^1P^o$ EIE cross section is in Reisenfeld *et al.* [7]. All uncertainties, systematic and statistical, were taken to be of random sign and uncorrelated, and were added in quadrature to determine the total experimental uncertainty.

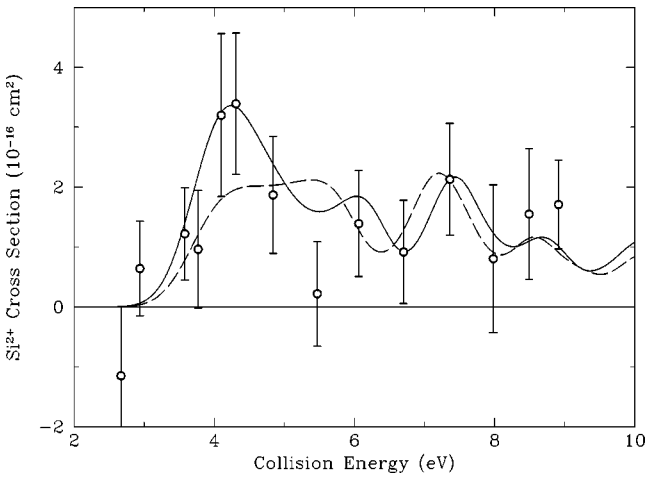

FIG. 5. Absolute energy-averaged EIE cross section for the Si^{2+} ($3s3p\ ^3P^o \rightarrow 3s3p\ ^1P^o$) transition. The error bars shown represent the total experimental uncertainty at a 90% confidence level. The highest-energy point includes a contribution from the $3s3p\ ^3P^o \rightarrow 3p^2\ ^3P$ excitation, which has a threshold of 9.54 eV. The solid and dashed curves show the 12-state close-coupling *R*-matrix calculation of Griffin, Pindzola, and Badnell [13] and the 45-state close-coupling *R*-matrix calculation of Griffin, Badnell, Pindzola, and Shaw [26], respectively, convolved with the experimental energy spread, which ranges from 0.85 eV (FWHM) at the lowest energies to 0.56 eV (FWHM) at the highest.

III. RESULTS AND DISCUSSION

Our absolute measurement of the energy-averaged $^3P^o \rightarrow\ ^1P^o$ EIE cross section is presented in Fig. 5. The error bars on the data points represent total experimental uncertainty at a 90% confidence level.

Although light is collected from over one quarter of the

total solid angle of the interaction region, the experiment is still sensitive to the angular distribution of the emitted photons. The most extreme values for the photon anisotropy arise from assuming that the excitation process results in light polarized parallel to the relative velocity vector ($\mathcal{P}=+1$), or perpendicular to it ($\mathcal{P}=-1$), which changes the fraction of photons collected by a factor of 1.21 or 0.90, respectively. In cases where autoionizing resonances contribute a large part of the total cross section, the degree of polarization can vary rapidly as a function of collision energy [27]. We do not include in the experimental uncertainty the error introduced by not accounting for the radiation anisotropy.

Also plotted are the 12-state close-coupling *R*-matrix calculation of Griffin, Pindzola, and Badnell [13] and the 45-state close-coupling *R*-matrix intermediate-coupling frame transformation (ICFT) calculation of Griffin, Badnell, Pindzola, and Shaw [26], shifted in energy so that the excitation threshold agrees with spectroscopic observations. Both calculations are convolved with the experimental energy distribution, which is represented as a 0.85-eV FWHM Gaussian at the lowest energies and a 0.56-eV FWHM Gaussian at the highest energies. The energy spread is interpolated between these two distributions at intermediate energies. Note that the conclusions drawn from the comparison of theory to experiment are insensitive to the choice of energy spread within the range of uncertainty.

Overall, the 12-state close-coupling calculation appears in good agreement with the experimental results both in the location and scale of the resonances, within experimental uncertainty and within the resolution allowed by the experimental energy spread. There is a suggestion that the calculation overestimates the cross section around 5.5 eV. Agreement with 12-state close-coupling calculations for the three other measured EIE cross sections in Si^{2+} has also been good [7,28]. Agreement with the larger, more sophisticated 45-state ICFT calculation is good except at threshold; it is possible that shifting the theoretical energy levels to match spectroscopic observations may improve the agreement [10]. There is no reason to expect better agreement with the 12-state calculation than with the 45-state calculation.

Measurements of the $^1S \rightarrow {}^3P^o$ transition in isoelectronic Ar^{6+} do not agree with the 8-state close-coupling calculations at threshold [12], and going down one *n* level, Bannister *et al.* measured a resonance in the $^3P^o \rightarrow {}^1P^o$ transition in C^{2+} that is not predicted by the 6-state close-coupling theory [8], suggesting that more work remains to be done.

IV. SUMMARY

We have determined the absolute cross section for electron-impact excitation of $Si^{2+}(3s3p\ ^3P^o \rightarrow 3s3p\ ^1P^o)$ for energies in the range 2.6–8.9 eV. The fraction of metastable $Si^{2+}(3s3p\ ^3P^o)$ in the beam was determined to be 0.256 ± 0.035 at 90% confidence. The measured resonance structure and absolute scale of the excitation are in good agreement with 12-state close-coupling *R*-matrix calculations [13] and somewhat worse agreement with 45-state close-coupling *R*-matrix calculations [26].

ACKNOWLEDGMENTS

The authors thank A. Daw, D. Griffin, and W. H. Parkinson for stimulating discussions. The authors also thank F. P. Rivera for technical assistance. This work was supported by NASA Supporting Research and Technology Program in Solar Physics Grant Nos. NAGW-1687 and NAG5-5059, and by the Smithsonian Astrophysical Observatory.

[1] J.L. Linsky, B.E. Wood, P. Judge, A. Brown, C. Andrulis, and T.R. Ayres, Astrophys. J. **442**, 381 (1994).
[2] D.J. Pinfield *et al.*, Astrophys. J. **527**, 1000 (1999).
[3] A. Ciaravella *et al.*, Astrophys. J. **529**, 575 (2000).
[4] F.P. Keenan, P. Dufton, and A.E. Kingston, Sol. Phys. **123**, 33 (1989).
[5] G.A. Doschek, U. Feldman, J.M. Laming, H.P. Warren, U. Schüle, and K. Wilhelm, Astrophys. J. **507**, 991 (1998).
[6] D.H. Crandall, R.A. Phaneuf, and G.H. Dunn, Phys. Rev. A **11**, 1223 (1975).
[7] D.B. Reisenfeld, L.D. Gardner, P.H. Janzen, D.W. Savin, and J.L. Kohl, Phys. Rev. A **60**, 1153 (1999).
[8] M.E. Bannister *et al.*, Int. J. Mass. Spectrom. **192**, 39 (1999).
[9] D.C. Griffin, M.S. Pindzola, F. Robicheaux, T.W. Gorczyca, and N.R. Badnell, Phys. Rev. Lett. **72**, 3491 (1994).
[10] T.W. Gorczyca, M.S. Pindzola, N.R. Badnell, and D.C. Griffin, Phys. Rev. A **51**, 488 (1995).
[11] T.W. Gorczyca, F. Robicheaux, M.S. Pindzola, and N.R. Badnell, Phys. Rev. A **52**, 3852 (1995).
[12] Y.-S. Chung, N. Djurić, B. Wallbank, G.H. Dunn, M.E. Bannister, and A.C.H. Smith, Phys. Rev. A **55**, 2044 (1997).
[13] D.C. Griffin, M.S. Pindzola, and N.R. Badnell, Phys. Rev. A **47**, 2871 (1993).
[14] C.E. Moore, *Atomic Energy Levels*, Natl. Bur. Stand. (U.S.) Circ. No. 35 (U.S. GPO, Washington, DC, 1971), Vol. 1.
[15] H.B. Gilbody, in *International Conference on Low Energy Ion Beams* (Institute of Physics, Bristol, UK, 1978), Vol. 38, p. 156.
[16] F. Aumayr and H. Winter, Phys. Scr., T **28**, 96 (1989).
[17] G.P. Lafyatis, Ph.D. thesis, Harvard University, 1982 (unpublished).
[18] M. Vujović, M. Matić, B. Čobić, and Y.S. Gordeev, J. Phys. B **5**, 2085 (1972).
[19] C.R. Tilford, J. Vac. Sci. Technol. A **1**, 152 (1983).
[20] H.S. Kwong, B.C. Johnson, P.L. Smith, and W.H. Parkinson, Phys. Rev. A **27**, 3040 (1983).
[21] G.P. Lafyatis, J.L. Kohl, and L.D. Gardner, Rev. Sci. Instrum. **58**, 383 (1987).
[22] D.B. Reisenfeld, Ph.D. thesis, Harvard University, 1998 (unpublished).
[23] M. Liehr, R. Trassl, M. Schlapp, and E. Salzborn, Rev. Sci. Instrum. **63**, 2541 (1992).

[24] W.T. Rogers, J.O. Olsen, and G.H. Dunn, Phys. Rev. A **18**, 1353 (1978).

[25] P.H. Janzen, Ph.D. thesis, Harvard University, 2002 (unpublished).

[26] D.C. Griffin, N.R. Badnell, M.S. Pindzola, and J.A. Shaw, J. Phys. B **32**, 2139 (1999).

[27] J. Mitroy, D.C. Griffin, D.W. Norcross, and M.S. Pindzola, Phys. Rev. A **38**, 3339 (1988).

[28] B. Wallbank, N. Djurić, O. Woitke, S. Zhou, G.H. Dunn, A.C.H. Smith, and M.E. Bannister, Phys. Rev. A **56**, 3714 (1997).